Evaluation of SPECT imaging: a multi-center and multi-vendor phantom study

Maria Inês Rebelo Gonçalves (mariairg.eb@gmail.com)
ISEL - Instituto Superior de Engenharia de Lisboa, Instituto Politécnico de Lisboa
Rui Parafita
Champalimaud Clinical Centre, Champalimaud Foundaton
Mauro Costa
Champalimaud Clinical Centre, Champalimaud Foundation
Ana Geão
Hospital CUF Descobertas
Edgar Pereira
Nuclearmed, HPA - Hospital Particular de Almada
Lina Vieira
H&TRC - Health & Technology Research Center, ESTeSL - Escola Superior de Tecnologia da Saúde, Instituto Politénico de Lisboa

Research Article

Keywords: SPECT, Spatial resolution, Sensitivity, Noise, Contrast, Image reconstruction, Standardization

Posted Date: December 29th, 2022

DOI: https://doi.org/10.21203/rs.3.rs-2347441/v1

RESEARCH

Evaluation of SPECT imaging: a multi-center and multi-vendor phantom study

Maria I.R. Gonçalves[1*], Rui Parafita[2,3], Mauro Costa[2], Ana Geão[3], Edgar Pereira[4], Lina Vieira[5]

[*] Correspondence: mariairg.eb@gmail.com
[1] ISEL - Instituto Superior de Engenharia de Lisboa, Insituto Politécnico de Lisboa, 1959-007 Lisbon, Portugal
Full list of author information is available at the end of the article

Abstract

Background: Single-photon emission computed tomography (SPECT) is a nuclear medicine (NM) imaging method sensitive for the evaluation and quantification of physiological processes in patients. However, there are different factors that affect qualitatively and quantitatively the SPECT images and, consequently, the reliability of the data. There is a degree of variability underlying the intrinsic performance of systems from the same or different manufacturers. In addition, the different configurations of the gamma cameras (GC) and the acquisition and reconstruction protocols used may lead to heterogeneity of results. This study compared SPECT images acquired in three GC from three NM centers, using the Jaszczak and NEMA IEC Body phantoms, filled with homogeneous solution of technetium-99m. Acquisitions were performed in each GC, following the protocols used in clinical practice of the respective NM center, and the images were analyzed and compared in terms of spatial resolution, sensitivity, noise, contrast, and contrast recovery (CR). Subsequently, the processing and reconstruction parameters were harmonized to assess their impact on the standardization of results.

Results: With the clinical protocols, the images acquired with the three GC showed small differences in spatial resolution, noise, and contrast, with the greatest difference being observed in the quantitative accuracy, since the CR has achieved variabilities of 0.17 and 0.28, for different activity concentrations. This intersystem variability was reduced to 0.09 and 0.08 after reconstruction algorithm standardization. However, this change increased the differences in the contrast percentage.

Conclusion: GC from different manufacturers showed the greatest heterogeneity of results, however, by eliminating possible sources of variation it is possible to reduce the differences between systems. It was demonstrated the need to include different parameters for the evaluation and comparison of SPECT images, so that procedures can be established between the different NM centers to ensure a trade-off between the various parameters assessed here, as the improvement of some usually leads to the deterioration of others.

Keywords: SPECT, Spatial resolution, Sensitivity, Noise, Contrast, Image reconstruction, Standardization.

Background

It is essential to ensure the acquisition of single-photon emission computed tomography (SPECT) images with the maximum accuracy for diagnosis, staging and evaluation of response to therapy, being of great importance to study the different factors that affect, qualitatively and quantitatively, the SPECT images [1].

The qualitative evaluation of SPECT images involves a visual interpretation, being dependent on the experience of the observer, as well as on the complexity of the human visual system, so it consists of a subjective method of image quality characterization. On the other hand, the quantitative evaluation of the image comprises objective methods of characterizing its quality, since it is based on measurements, for example, of the noise and contrast of the SPECT image [2]. However, there are several factors which degrade the image quality and, consequently, the reliability of quantitative data, and they can be grouped into instrumental factors (associated with the performance of the equipment components), physical factors (resulting from the interaction between radiation and matter [3]) and physiological factors (associated to the patient's biology and physiology) [4].

Although in the last decades, there has been a growing concern with the SPECT image quality, both qualitatively and quantitatively, and consequently with the development of methods of correction of the factors which degrade the image quality, the clinical adoption of these methods has been slow [5]. Thus, although the instrumentation inherent to the GC has not undergone significant changes along the years, further studies are necessary regarding the image quality provided by different equipment. There has been observed a degree of variability underlying the intrinsic performance of systems from the same or different manufacturers [6], which may represent a significant influence in diagnostic procedures since the different configurations of the GC and the acquisition, reconstruction and post-processing protocols utilized [7], may lead to distinct results [8]. Thus, to ensure that comparable SPECT image data are obtained, the harmonization of protocols and procedure guidelines between different GC is fundamental.

In 2009, Hughes et al. [9] compared the spatial resolution of three SPECT/CT systems, concluding that it is strongly dependent on the reconstruction algorithm, and in 2012, in another study [10], they compared the image quality of the same three systems for cardiac applications, demonstrating that they performed differently in terms of quantitative accuracy, contrast, SNR and uniformity.

Thus, although the harmonization of SPECT protocols between different GC is not yet a widely explored area of research in a multicenter environment, more recently some studies have been carried out using phantoms [5,11–14], with the main objective of assessing what extent the different GC configurations and acquisition, reconstruction and processing protocols can influence, qualitatively and quantitatively, the quality of the image obtained. A study by Zimmerman et al. [5] confirmed the need for detailed and harmonized acquisition and processing protocols among different institutions to achieve accurate and reliable quantification, as they found a significant variation of results in the quantification performed at different sites. Subsequently, studies by Peters et al. [11] and Kupitz et al. [13] have shown that differences in reconstruction protocols have a greater influence on the variability between different GC and NM centers in terms of quantitative accuracy.

The evidence has demonstrated the existence of controversies in the quality of SPECT images obtained in different conditions, whether in different GC, in a multicentric environment, or in images acquired with the same equipment and in the same place but following different guidelines. In addition to the differences in the electronics associated with each GC model, the different procedures inherent to the acquisition, reconstruction, and processing of the studies may be at the basis of the diversity of results evidenced. Therefore, there is a need to standardize and optimize the protocols and procedures guidelines to achieve better values in quantitative accuracy and repeatability of results in different NM centers, so that the data obtained can be reliably compared.

The European Association of Nuclear Medicine (EANM) has created the EARL

Accreditation program for positron emission tomography/computed tomography (PET/CT) [15], allowing the standardization in a multicenter environment of the quantification of the most widely used radiopharmaceutical in PET, fluorodeoxyglucose (^{18}F-FDG). Thus, the establishment of a similar program would allow greater standardization of procedures and consequently improve the alignment of quantification between different systems, greater insight into the quantitative accuracy and precision, as well as the performance of different equipment, is required.

This study aims to compare qualitatively and quantitatively the SPECT images obtained in three GC from three NM centers, using the Jaszczak and NEMA IEC Body phantoms.

Methods

Phantoms

Phantom measurements were performed using a Jaszczak (Deluxe Jaszczak Phantom™) [16] and a NEMA IEC Body (NEMA IEC Body Phantom Set™) [17] phantoms.

The Jaszczak used has a background compartment volume of approximately 5.7 litres (with inserts), six cold spheres representing various lesion sizes with diameters of 9.5, 12.7, 15.9, 19.1, 25.4 and 31.8 mm, and six sets of cold rods with diameters of 4.8, 6.4, 7.9, 9.5, 11.1 and 12.7 mm. This phantom allows to easily access spatial resolution, computation of the contrast for cold lesions, noise, and volumetric sensitivity of the systems. The standard NEMA IEC Body phantom contains a compartment with a volume of 9.28 litres (with inserts) and six fillable spheres with inner diameters (and corresponding volumes) of 10 mm (0.52 ml), 13 mm (1.15 ml), 17 mm (2.57 ml), 22 mm (5.57 ml), 28 mm (11.49 ml) and 37 mm (26.52 ml). This phantom is useful for quantitative image analysis, by determining the contrast recovery in the hot spheres, providing the comparison of different GC models in terms of quantitative accuracy.

The phantoms were filled with ^{99m}Tc diluted in water. For the NEMA IEC Body, two syringes with the same activity were used, one of them being injected directly into the background compartment of the phantom (previously filled with water), and the activity of the other syringe was diluted in 1 litre of water and then injected into each of the six spheres. The lung insert of this phantom was not filled.

Acquisitions were performed with both phantoms, in each NM center, for 370 and 740 MBq activities and, therefore, activity concentrations of 0.06 and 0.13 MBq/mL in the Jaszczak phantom, and a spheres-to-background ratio approximately equal to 9.4:1 in the NEMA phantom. At the acquisition time, the activity in the phantoms ranged between 321 and 366 MBq and between 681 and 752 MBq.

Gamma Cameras

Three gamma cameras from two manufacturers were included in this study: a Philips BrightView (Philips Healthcare), a GE NM/CT 850, and a GE Infinia II (GE Healthcare) (Table 1).

Table 1 Main properties of all used dual-headed gamma cameras, with LEHR* collimator

System	Philips BrightView	General Electrical NM/CT 850	General Electrical Infinia II
Detector Crystal	3/8″ NaI	5/8″ NaI	3/8″ NaI
PMT**	59	59	59
FOV***	54 x 40.6 cm	54 x 40 cm	54 x 40 cm
Hole shape	Hexagonal	Hexagonal	Hexagonal
Collimator hole diameter	1.22 mm	1.5 mm	1.5 mm

Hole length	27 mm	35 mm	35 mm
Septal thickness	0.152 mm	0.2 mm	0.2 mm
Septal penetration @ 140 keV	1.7%	0.3%	0.3%

**LEHR* low-energy high-resolution, ***PMT* photomultiplier tube, ****FOV* field of view

Data Acquisition

To compare the image quality between systems and evaluate the trend of each GC, images of each phantom were acquired, following the acquisition parameters of the bone SPECT protocol used in clinical practice of the respective NM center. Thus, in each NM center, two acquisitions were performed with each phantom. The SPECT acquisition settings are detailed in Table 2.

Table 2 SPECT acquisition parameters

System	Philips BrightView	GE NM/CT 850	GE Infinia II
Collimator	LEHR	LEHR	LEHR
Acquisition mode	Step and shoot	Step and shoot	Step and shoot
Arc of rotation	360º	360º	360º
Matrix size	128 x 128	128 x 128	128 x 128
Projections number	128	60	72
Projection time	15 s	16 s	25 s
Zoom factor	1.0	1.0	1.0
Energy window	144 keV (±10%)	140 keV (±10%)	140 keV (±10%)

In addition to SPECT, CT acquisitions were performed, providing an anatomical reference of the phantoms, to assist the segmentation of the regions of interest (ROI). This was done in the CT component of the GE NM/CT 850 gamma camera or an external CT. In all cases, the SPECT and CT images were co-registered.

Data Reconstruction

Firstly, the images acquired with the Jaszczak and NEMA IEC Body phantoms were processed and reconstructed, in the respective NM center, according to the software and parameters used in clinical practice (Table 3).

Table 3 SPECT reconstruction parameters

System	Philips BrightView	GE NM/CT 850	GE Infinia II
Reconstruction	Astonish	OSEM*	OSEM
Iterations	2	2	2
Subsets	16	10	10
Pre-reconstruction filter	None	Hann (0.9 cycles/pixel)	Hann (0.9 cycles/pixel)
Post-reconstruction filter	None	Butterworth (0.48 cycles/pixel, order 10)	Butterworth (0.48 cycles/pixel, order 10)
Image voxel size	4.664 x 4.664 x 4.664 mm^3	4.418 x 4.418 x 4.418 mm^3	4.428 x 4.428 x 4.428 mm^3

**OSEM* ordered subset expectation maximization

Subsequently, considering the analysis of the images acquired and processed following the clinical protocols, the reconstruction parameters were reformulated to investigate the influence of their standardization on image quality and on the reproducibility of values between different GC and MN centers.

For this purpose, the reconstruction method (OSEM) and the number of subsets (16) were equalized in all the images acquired in the three GC. The IntelliSpace Portal 11.0, available on the Philips BrightView processing station, does not allow the applying of pre-reconstruction filters for OSEM, so it was initially chosen to process the images only with the Butterworth post-reconstruction filter, with a cutoff frequency of 0.48 cycles/pixel and order 10 (Protocol 1), as already defined in the other GC. Next, another parameterization was tested, in which no filters were applied (Protocol 2). These new reconstruction and processing parameters analyzed in this study are presented in Table 4.

Table 4 Examined reconstruction protocols

Protocol	1	2
Reconstruction	OSEM	OSEM
Iterations	2	2
Subsets	16	16
Post-reconstruction filter	Butterworth (0.48 cycles/pixel, order 10)	None

Image analysis

Jaszczak SPECT images were analyzed qualitatively, in terms of spatial resolution, and quantitatively, by determining volumetric sensitivity, percentage of contrast, and noise.

The images from the NEMA IEC Body were used to calculate contrast recovery (CR) as determined by the NEMA NU 2-2018 standard [18], to compare the quantification at different GC and thus evaluate the reproducibility of the values.

Spatial resolution

Spatial resolution (in mm) was obtained, subjectively, through visual interpretation. For that, the smallest space visible and recognizable among the set of rods in the SPECT image was considered its spatial resolution.

Sensitivity

The software 3D Slicer 4.11 [19] was used to create a mask in the Jaszczak's uniform section on a CT of the phantom, which was subsequently applied to each of its SPECT images, to obtain the value of the total counts in the segmented volume of interest (VOI) (Figure 1).

The sensitivity (S) was calculated by equation (1):

$$S = \frac{N_{VOI}/V_{VOI}}{A \times t} \quad (1)$$

Where N_{VOI} is the total number of counts in the volume of interest (V_{VOI}), A is the actual activity concentration in the phantom and t is the acquisition time, corresponding to the number of projections multiplied by the time per projection.

Noise

The SPECT images noise was determined by using the data extracted from 3D Slicer after segmentation of a cylindrical VOI in the Jaszczak's uniform section (Figure 1).

The noise was calculated by the ratio of the standard deviation (SD_{VOI}) and the mean value of counts ($\bar{N}_{VOI}$) in the VOI:

$$N\,[\%] = \frac{SD_{VOI}}{\bar{N}_{VOI}} \times 100 \tag{2}$$

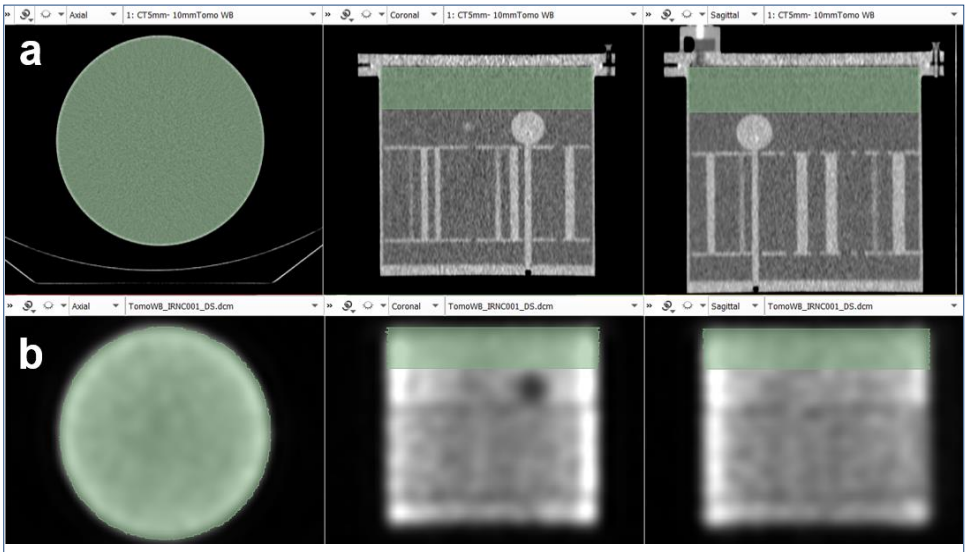

Figure 1. Example of the segmentation performed in the Jaszczak images, in the axial, coronal and sagittal planes, for sensitivity and noise determination. **(a)** Mask created on CT data. **(b)** Mask applied to SPECT images

Contrast

To calculate the contrast between the cold spheres and the background, a mask was created in a Jaszczak CT, where VOIs were segmented in each of the six spheres, according to their known diameter. Then, 6 VOIs were drawn on the background, with the same diameter as the largest sphere (31.8 mm). The mask was then applied to each of the SPECT images (Figure 2).

The contrast (C) was calculated by equation (3):

$$C\,[\%] = \frac{\bar{N}_{Bg} - \bar{N}_{VOI,j}}{\bar{N}_{Bg}} \times 100 \tag{3}$$

Where $\bar{N}_{Bg}$ and $\bar{N}_{VOI,j}$ are the average counts in the background and in the VOI for sphere j.

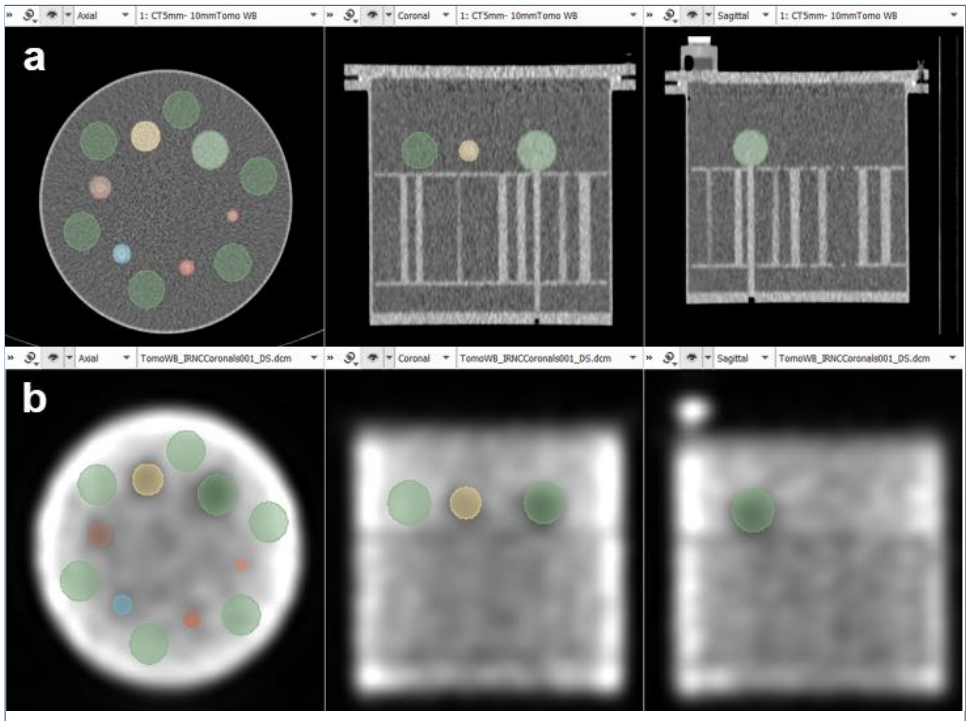

Figure 2. Example of the segmentation performed on the Jaszczak images, in the axial, coronal and sagittal planes, for contrast determination. **(a)** Mask created on CT data. **(b)** Mask applied to SPECT images

Contrast recovery coefficients

To calculate the contrast recovery in the hot spheres, a mask was created in a NEMA IEC body CT, which was then transferred to each co-registered reconstructed SPECT. As shown in Figure 3, spherical VOIs were initially defined for all six hot spheres, with a diameter of 40 mm. The spheres' final VOIs were obtained by applying a 50% threshold of the sphere maximum voxel value after correction for the background activity:

$$VOI_{tresh,j} = 0.5\ (VOI_{max,j} + VOI_{mean,Bg}) \tag{4}$$

Where $VOI_{tresh,j}$ is the threshold value for the sphere j VOI, $VOI_{max,j}$ is the maximum value of the counts in the VOI of the sphere j and $VOI_{mean,Bg}$ is the average counts in the background VOIs. Mean background counts was accessed after placing 12 VOIs with identical diameter in the background of the phantom, but in a bottom slice, to avoid the influence of sphere counts on the average background counts.

The CR for each hot sphere was determined using equation (5), where $\overline{N}_{VOI,j}$ is the average counts in the VOI for sphere j, $\overline{N}_{Bg}$ is the average of the background VOI counts and A_{VOI} and A_{Bg} are the activity concentrations in the hot spheres and in the background, respectively [18]:

$$CR = \frac{\left(\overline{N}_{VOI,j} \Big/ \overline{N}_{Bg}\right) - 1}{\left(A_{VOI} \Big/ A_{Bg}\right) - 1} \tag{5}$$

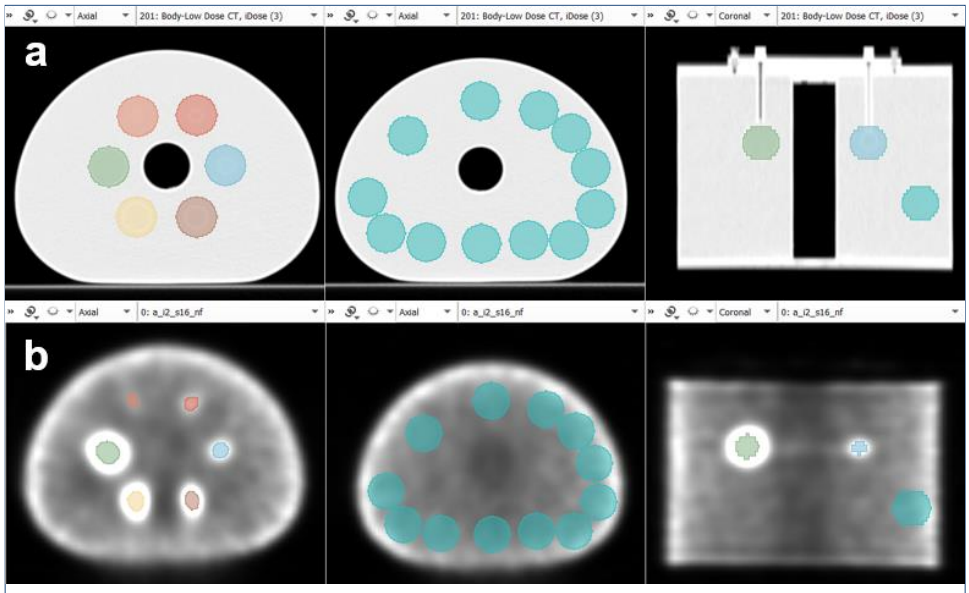

Figure 3. Example of the segmentation performed on the NEMA IEC body phantom images, for contrast recovery determination. **(a)** Mask developed on CT data. **(b)** Mask applied to SPECT images

Intersystem variability

The intersystem variability of contrast and CR was assessed, for each sphere, by the range of the values over all systems according to [12]:

$$Range_j = C_{j,max} - C_{j,min} \quad (6)$$

Where $C_{j,max}$ and $C_{j,min}$ are, respectively, the maximum and minimum contrast/CR values found over the three systems for sphere j.

Similarly, the variability of sensitivity and noise between systems was also calculated by the range of the values found over all systems.

Results

Qualitative results

Spatial resolution

With the clinical acquisition and reconstruction protocols (Figure 4), the spatial resolution differed between the three GC. For 370 MBq, with Philips BrightView it is possible to detect partially the 12.7 mm set of rods, whereas GE NM/CT allows a distinction of the 12.7 mm rod set and partially the 11.1 mm set of rods. At GE Infinia's image, the 12.7 and 11.1 mm rods sets are clearly distinguishable and de 9.5 mm set is partially perceptible.

With the increase of activity to 740 MBq, the images acquired with Philips BrightView and GE NM/CT became sharper, and it was possible to observe rods of smaller diameter (up to 11.1 mm). The GE Infinia's image kept the spatial resolution.

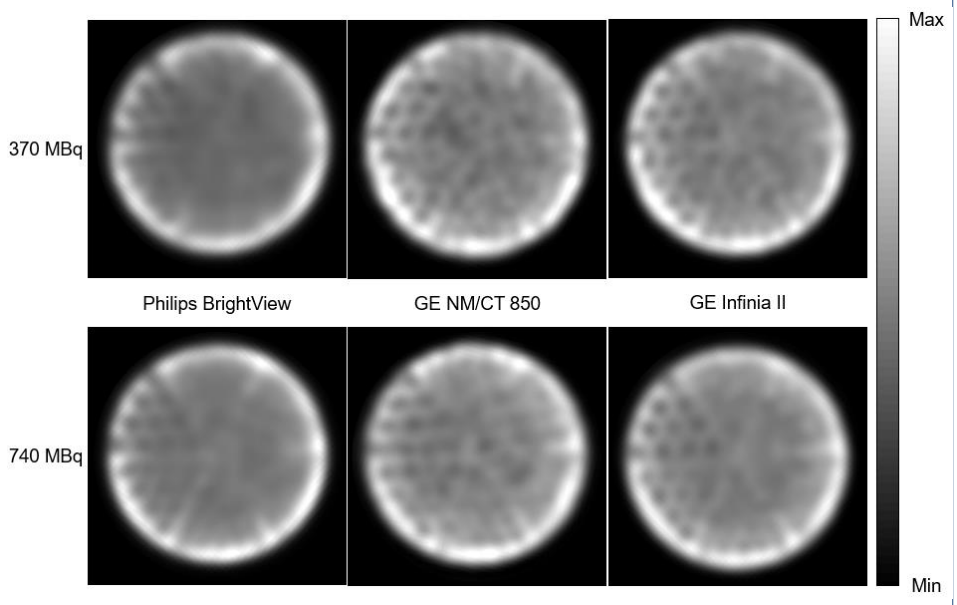

Figure 4. SPECT images of the Jaszczak phantom for all systems, acquired and reconstructed with respective clinical protocols, for spatial resolution evaluation

After standardizing the reconstruction parameters between systems (Figure 5), there was an improvement in sharpness of the images acquired with Philips BrightView and Infinia and reconstructed by protocol 1. For 370 MBq, with Philips BrightView it became possible to clearly distinguish the rods up to 11.1 mm, whereas Infinia allows a clear distinction of the 11.1 mm rod set and partially up to 9.5 mm. With NM/CT was possible to distinguish the rods up to 11.1 mm. The images reconstructed with protocol 2 presented very poorer spatial resolution, inadequate for clinical applications.

With the increase of activity, the spatial resolution slightly improved for all the systems.

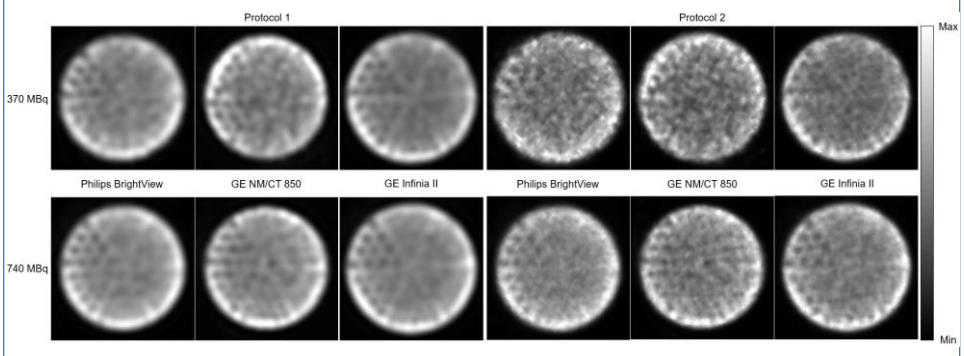

Figure 5. SPECT images of the Jaszczak phantom for all systems, acquired and reconstructed with protocols 1 and 2, for spatial resolution evaluation

Quantitative results

Sensitivity

With the clinical acquisition and reconstruction protocols, for 370 MBq the sensitivity of the GC (Table 5) is between 22.06 and 22.31 cps/MBq, corresponding to a variability range of 0.25 cps/MBq. The increase of activity led to a slight decrease of sensitivity in the three

GC and the variability increased to 1.59 cps/MBq.

After applying different reconstruction parameters, the values determined for sensitivity remained practically unchanged but, when the reconstruction protocol 2 was applied to the Philips BrightView images, calculated sensitivity was significantly reduced.

Table 5 Sensitivity values for data acquired with different ^{99m}Tc activities and reconstructed with different protocols (clinical, 1 and 2)

^{99m}Tc activity	Protocol	Sensitivity [cps/MBq]		
		Philips BrightView	GE NM/CT 850	GE Infinia II
370 MBq	Clinical	22.06	22.31	22.23
	1	20.83	22.41	22.33
	2	10.43	22.48	22.39
740 MBq	Clinical	21.85	20.25	21.49
	1	20.65	20.30	21.54
	2	10.34	20.37	21.59

Noise

With the clinical acquisition and reconstruction protocols, for 370 MBq the noise of the images acquired with different GC (Table 6) varied 3.34%. When used the activity of 740 MBq this range increased.

The images acquired with Philips BrightView and reconstructed with protocol 1 showed less noise than those which had been reconstructed with the clinical parameters. However, the images acquired with GC from GE presented a slight increase of noise when reconstructed with protocols 1 or 2.

Table 6 Percent noise of images acquired with different ^{99m}Tc activities and reconstructed with different protocols (clinical, 1 and 2)

^{99m}Tc activity	Protocol	Noise [%]		
		Philips BrightView	GE NM/CT 850	GE Infinia II
370 MBq	Clinical	28.00	25.82	24.66
	1	25.57	26.76	24.78
	2	28.94	32.49	27.30
740 MBq	Clinical	29.16	29.12	24.43
	1	26.42	29.62	24.77
	2	27.99	32.38	26.10

Contrast

With the clinical protocols, for all systems, the contrast between cold spheres and background increased with increasing sphere diameter (Figure 6).

For 370 MBq (Figure 6d), the largest intersystem variability (≈ 7%) was observed in the 15.9 mm sphere. Figure 6e demonstrates that, in general, the contrast values calculated for 740 MBq present less intersystem variability, with a maximum range of approximately 4% (19.1 and 31.8 mm spheres).

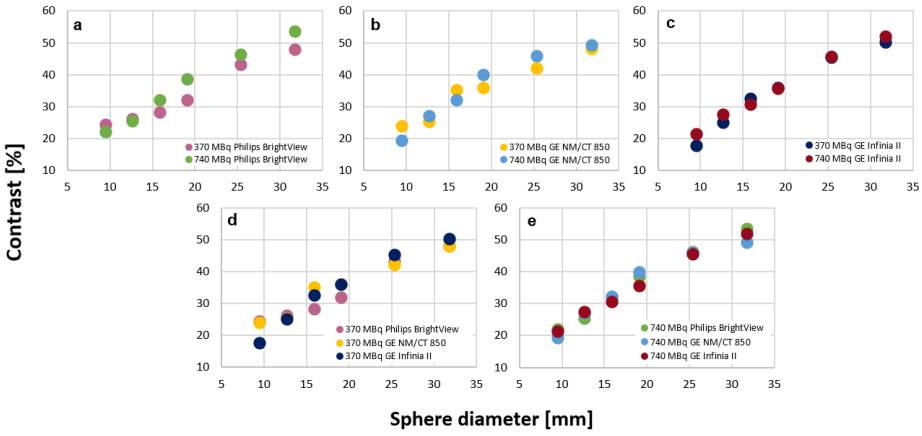

Figure 6. Contrast as a function of sphere diameter for all systems separately (**a-c**), and for all systems combined (**d-e**), for data acquired (370 and 740 MBq) and reconstructed with respectively clinical protocols. (**a**) Philips BrightView, (**b**) GE NM/CT 850, (**c**) GE Infinia II, (**d**) Contrast values for all systems combined, for 370 MBq, (**e**) Contrast values for all systems combined, for 740 MBq

The reconstruction of the images acquired with Philips BrightView using different parameters had an influence on the contrast. For 370 MBq (Figure 7a), the greatest differences compared with clinical protocol were found for the smallest sphere, where the contrast increased with the new reconstruction protocols. For 740 MBq (Figure 7d), the greatest variation caused by both protocols occurred for the 12.7 mm sphere, in which the contrast decreased. On the other hand, the images acquired with GE NM/CT and Infinia showed higher contrast values when reconstructed with protocols 1 or 2 (Figure 7b-c, e-f).

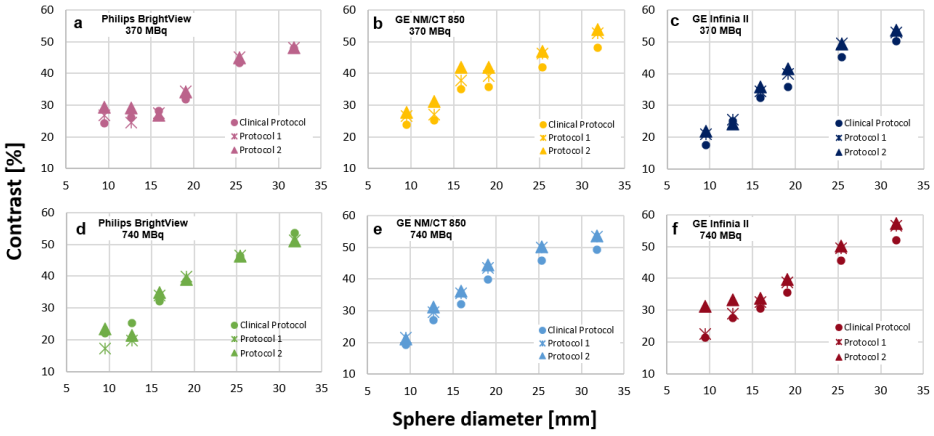

Figure 7. Contrast as a function of sphere diameter for data acquired with different ^{99m}Tc activities and reconstructed with different protocols (clinical, 1 and 2). (**a**) Philips BrightView (370 MB), (**b**) GE NM/CT 850 (370 MBq), (**c**) GE Infinia II (370 MBq), (**d**) Philips BrightView (740 MBq) (**e**) GE NM/CT 850 (740 MBq), (**f**) GE Infinia II (740 MBq)

Contrast recovery coefficients

With the clinical protocols, CR increased with increasing sphere diameter for each system (Figure 8). By analyzing the quantitative accuracy of each GC for different ^{99m}Tc activities, CR values are quite similar (Figure 8a-c). However, in the images acquired with Philips BrightView (Figure 8a), the calculated CR for the 28 mm sphere was higher in the image acquired with 740 MBq.

When comparing the contrast recovery between the systems (Figure 8d-e), the CR values are considerably higher, in the two largest spheres, for the images acquired with Philips BrightView. For 370 MBq, the maximum intersystem variability was found in the largest sphere, with a range of 0.17. With increasing activity concentration, this variability range increased to 0.28, in the 28 mm sphere.

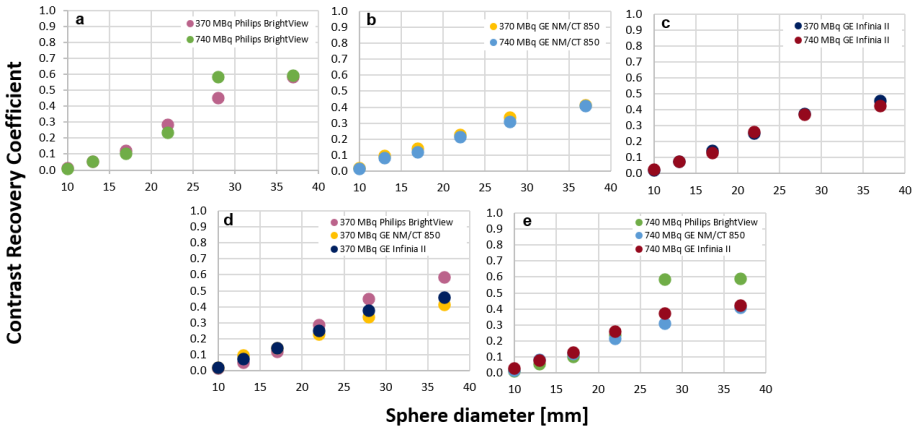

Figure 8. CR as a function of sphere diameter for all systems separately (**a-c**), and for all systems combined (**d-e**), for data acquired (370 and 740 MBq) and reconstructed with respectively clinical protocols. (**a**) Philips BrightView, (**b**) GE NM/CT 850, (**c**) GE Infinia II, (**d**) CR coefficients for all systems combined, for 370 MBq, (**e**) CR coefficients for all systems combined, for 740 MBq

The reconstruction protocols 1 and 2 applied to the images acquired with Philips BrightView led to a considerable decrease of CR in the two largest spheres (Figure 9a, d). When compared to clinical reconstruction, the image acquired with GE NM/CT, for 740 MBq, and reconstructed by protocol 1, resulted in an increase of CR (Figure 9e). This trend was also verified for the images acquired with Infinia II (Figure 9c, f). Protocol 2 represented greater influence on CR, leading to its increase in all spheres in the images acquired with NM/CT and Infinia.

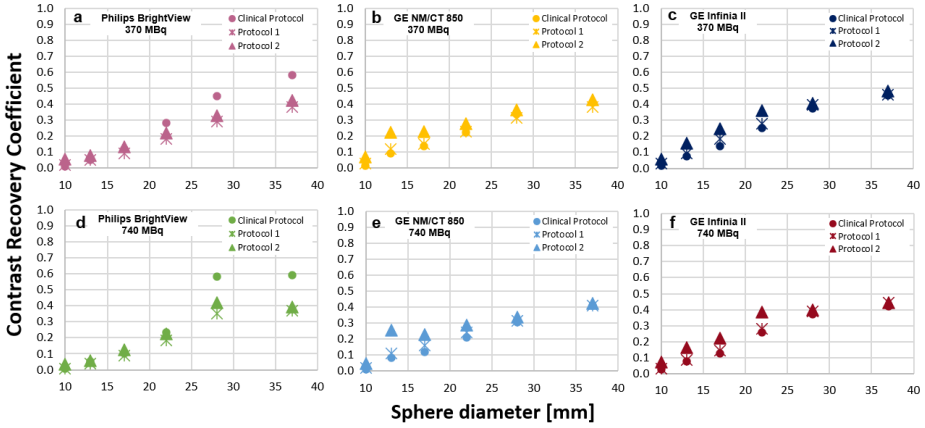

Figure 9. CR as a function of sphere diameter for data acquired with different ^{99m}Tc activities and reconstructed with different protocols (clinical, 1 and 2). (**a**) Philips BrightView (370 MB), (**b**) GE NM/CT 850 (370 MBq), (**c**) GE Infinia II (370 MBq), (**d**) Philips BrightView (740 MBq) (**e**) GE NM/CT 850 (740 MBq), (**f**) GE Infinia II (740 MBq)

Effect of reconstruction algorithm on intersystem variability

The intersystem variability was determined for the different quantitative image quality evaluation parameters. The results have been compared between GC, for the same protocol (clinical, 1 or 2) and for two different protocol combinations, which seemed to provide a better reproducibility of values in some parameters.

Although sensitivity depends essentially on the inherent characteristics of the GC and collimator used, for 370 MBq, the images reconstructed with clinical protocols showed the lowest intersystem variability (Figure 10a). With increasing activity, the lowest range between systems was obtained by applying protocol 1 to the three acquisitions (Figure 10b). Protocol 2 demonstrated the greatest heterogeneity in the calculated sensitivity values.

The intersystem variability of the noise was reduced from 3.34 to 1.17% by changing only the reconstruction parameters of 370 MBq Philips BrightView acquisition to those of the protocol 1 (Figure 10c). With the increase of activity concentration (Figure 10d), the lowest variability was found by applying the protocols 1 or 2 only to the SPECT image acquired with Philips BrightView.

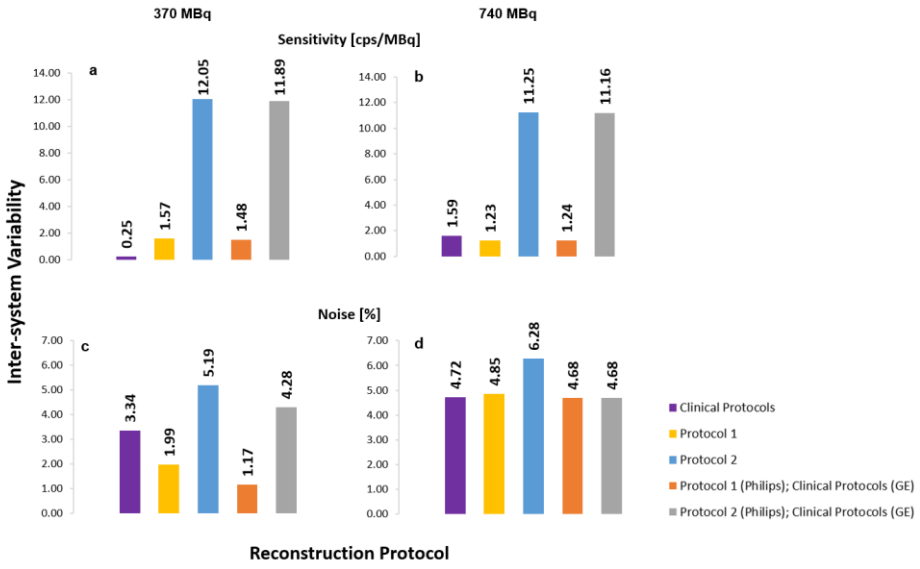

Figure 10. Comparison in range over all systems in sensitivity (**a-b**) and noise (**c-d**), for acquisitions of 370 MBq (**a, c**) and 740 MBq (**b, d**), as a function of the different reconstruction protocols analyzed

Figure 11a shows that, for 370 MBq acquisition, the clinical reconstruction protocols caused a maximum contrast intersystem variability of 6.94% (15.9 mm sphere). The standardization of reconstruction parameters, with protocols 1 and 2, increased this variability. Using the parameters of protocol 1 only to the Philips BrightView acquisition reduced the intersystem variability in the 12.7, 19.1 and 21.8 mm spheres, however, the maximum range of contrast increased in the smallest sphere.

For 740 MBq, there was a generalized decrease in the maximum variation between systems (Figure 11b). Here, it is observed that the clinical protocols resulted in a maximum range of contrast equal to 4.37% (19.1 mm sphere). Reconstructing only the image acquired with Philips BrightView according to the protocols 1 or 2 reduced the variability in the largest sphere, however the maximum intersystem variability increased in the 12.7 mm sphere.

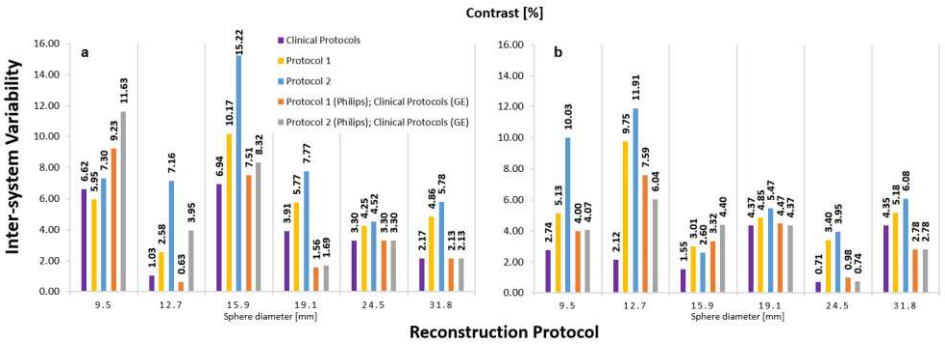

Figure 11. Comparison in range over all systems in contrast, for acquisitions of 370 MBq (**a**) and 740 MBq (**b**), as a function of the different reconstruction protocols analyzed

For 370 MBq acquisition, Figure 12a shows that the clinical reconstruction protocols resulted in a maximum CR intersystem variability of 0.17, in the largest sphere. It was possible to decrease the variability of CR in the largest sphere from 0.17 to 0.07 by changing only the reconstruction parameters in the Philips BrightView image to those established in protocol 1. Whit this change, the maximum variation was 0.09, in the 28 mm sphere.

Figure 12b shows that, with the increase of activity concentration, the clinical reconstruction protocols resulted in a maximum CR variability of 0.28 (28 mm sphere). By applying the protocol 1 only to the Philips BrightView image, this range decreased to 0.06, and the maximum variation between GC was 0.08, in the 22 mm sphere.

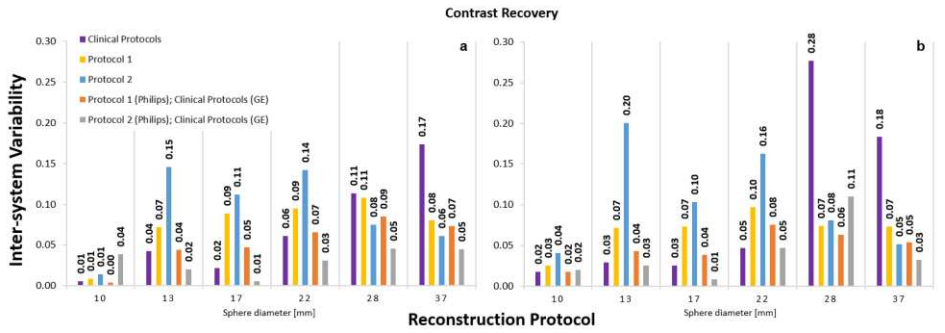

Figure 12. Comparison in range over all systems in CR, for acquisitions of 370 MBq (**a**) and 740 MBq (**b**), as a function of the different reconstruction protocols analyzed

Discussion

This study compared SPECT images acquired in three GC from two manufacturers, following their own clinical protocols, which differ in terms of number of projections and time per projection. The reconstruction protocols are the same in centers which have systems from the same manufacturer (GE), differing from center which have GC Philips BrightView in terms of reconstruction algorithm, total number of iterations and in the use of filters.

With the clinical protocols, the spatial resolution ranged between 12.7 and 9.5 mm and, although this parameter has been subjectively evaluated, GE Infinia have presented the best spatial resolution. These differences observed in spatial resolution may be due, primarily,

to factors inherent to the collimator-detector response, as well as to the septal penetration [20,21], since differences have been observed in the detection system of each GC. Also, the acquisition parameters influence the spatial resolution, because the number of projections should be at least equivalent to the matrix size [21,22], which in the present study has not been verified.

Furthermore, with Philips BrightView the reconstruction is performed with the manufacturer's algorithm (Astonish), using 2 iterations (i) and 16 subsets (s), and with GE systems the OSEM algorithm (2i/10s) is used. After replacing Astonish for OSEM reconstruction (protocol 1), the spatial resolution of the images acquired with Philips BrightView improved and became similar to that obtained with the other systems. This result is consistent with a study by Hughes et al. [9], where they found that using standardized algorithm, the images acquired with different GC showed identical spatial resolution. By using protocol 2 (OSEM, 2i/16s, no filter), there was an increase in the blurring artefact in all images, due to the absence of the Butterworth filter, which allowed the suppression of statistical noise, and simultaneously preserved the spatial resolution, as described by Lyra et al. [23]. Thus, it was found that there is a harmonization of the spatial resolution between GC using protocol 1 (OSEM, 2i/16s, Butterworth, 0.48 cycles/pixel, order 10).

The sensitivity of the GC did not change linearly with source activity but decreased when the detection system was submitted to a high-count rate, as sensitivity decreased in all GC with increasing activity concentration, which may be related to the dead time of the systems [24]. There is no evidence to support a correlation between sensitivity and reconstruction parameters of SPECT images, since this depends on the characteristics of each equipment and collimator used. Therefore, it is necessary to carry out further studies to understand the cause of the decrease observed in the mean counts in the images acquired with Philips BrightView and reconstructed with protocol 2.

In the images reconstructed with the clinical protocols, for 370 MBq, the noise was higher in the image acquired with Philips BrightView. This parameter is influenced by factors such as acquisition time, number of projections, energy window, and the total number of iterations [22], which may justify there being more similarity between the images acquired on the NM/CT and Infinia. With Philips BrightView, the total number of iterations was higher (32 versus 20), which itself increases the noise level, as observed in other studies by Kupitz et al. [13] and Alqahtani et al. [14].

The images acquired with Philips BrightView and reconstructed using protocol 1 (OSEM, 2i/16s, Butterworth, 0.48 cycles/pixel, order 10) showed less noise than those reconstructed with the clinical protocol, in contrast to what was seen in the images acquired with NM/CT and Infinia, which is consistent with the results found in previous studies [13,14], since increasing the total number of iterations implies an increase of noise. For the 740 MBq acquisition, protocol 2 (OSEM, 2i/16s, no filter) also led to a decrease of noise in the image acquired with Philips BrightView and an increase in the other images, which was due to the filtering suppression of the images acquired with NM/CT and Infinia, whose clinical processing included pre- and post-reconstruction filters. Thus, it was found that by reconstructing the studies acquired in Philips BrightView according to the protocol 1, and keeping the clinical protocols in the other GC, it was possible to approximate the value of the noise between the images.

The contrast between the cold spheres and the background tends to increase with the increase of activity concentration in the phantom, which agrees with what has been verified by Yusof et al. [25]. The contrast is lower than 100% in all the images, because of factors such as septal penetration and scattered radiation, which leads to contrast deterioration between regions with different levels of activity uptake [26,27], and also because of the spill-in phenomenon, evidenced by the overestimation of activity in the cold spheres as a consequence of the integration, in the respective VOIs, of the ^{99m}Tc concentration existing in the phantom background [28,29]. The partial volume effect mostly influenced the smaller

structures, as a decrease in contrast was observed with decreasing volume of the spheres, as in the results observed by Alqahtani et al. [14] and Yusof et al. [25], which demonstrates the increased difficulty in detecting cold lesions when they are smaller than 12.7 mm.

With the different reconstruction protocols, the increase in the total number of iterations from 20 to 32, in the images acquired with the GE NM/CT and Infinia, has allowed an increase in the contrast, as verified in the study by Alqahtani et al. [14]. Without post-reconstruction filtering, the contrast increased in the image acquired with GE NM/CT and Infinia. The results achieved with protocol 2 are similar to those of the study by Alqahtani et al. [14], who found that increasing the bandwidth of Gaussian filters led to a contrast decrease. Although the new reconstruction parameters originated a higher contrast between the cold spheres and the background, it was observed that this increase was relatively lower in the images acquired with Philips BrightView and, consequently, originated a higher heterogeneity of results. Therefore, it is necessary to understand the influence that the differences in the acquisition parameters, might be having on this parameter.

In this study, the quantitative accuracy of GC was evaluated by determining the CR values in the different spheres of the NEMA IEC Body phantom. Contrast recovery tends to increase with increasing sphere diameter, which is in accordance with previous studies [5,11–14,25], and it is a consequence of partial volume artifacts. In the two larger spheres, the calculated CR for Philips BrightView were considerably higher and closer to 1, so there was an increasing variability of CR values between GC, representing a maximum variation of 0.17 in images acquired with 370 MBq, and of 0.28 with increasing activity concentration. In the same two spheres, the maximum variability of CR between NM/CT and Infinia did not exceed 0.06, emphasizing the fact that quantitative precision is better between GC from the same manufacturer, as verified by Peters et al. [12]. The better quantitative accuracy obtained with Philips BrightView agrees with a study by Knoll et al. [30], where Astonish was shown to provide better absolute quantification when compared to standard OSEM.

Increasing the total number of iterations from 20 to 32 in the images acquired with the GE NM/CT and Infinia resulted in a generalized increase of CR values, as verified by other authors [13,14]. With protocol 2, it was confirmed that unfiltered reconstruction allowed for improved quantitative accuracy of the images acquired with GE NM/CT and Infinia, as suggested by Alqahtani et al. [14]. The protocol 2 applied to the images acquired with Philips BrightView resulted in a decrease of CR in the larger spheres and, considering that the only difference between this and clinical protocol is the reconstruction algorithm, it suggests that the abrupt increase in CR that was seen in the two larger spheres was probably related to the use of Astonish.

Conclusion

It was demonstrated the need to include different parameters for the evaluation and comparison of SPECT images so that procedures can be established between the different NM centers to ensure a trade-off between the various parameters assessed here, as the improvement of some usually leads to the deterioration of others. It was concluded that the best CR reproducibility was achieved by equalizing the reconstruction algorithm (OSEM, protocol 1), which decreased the maximum variability of CR values from 0.17 to 0.09, in the images acquired with 370 MBq, and from 0.28 to 0.08 in the 740 MBq acquisitions. Thus, by eliminating possible sources of variation, it was possible to improve the reproducibility of values between systems, however, the absolute quantification was compromised. Furthermore, by replacing the Astonish algorithm by OSEM, it was possible to standardize the results achieved between GC in terms of spatial resolution and noise. However, this change increased the differences observed in the percentage of contrast.

Since the GC from different manufacturers showed the highest heterogeneity of results

and, since after standardization of the reconstruction parameters, there continued to be differences in image quality in different GC models, it could be established that the processing and reconstruction hardware and software influence the intersystem variability.

List of abbreviations

2i/10s: 2 iterations and 10 subsets; 2i/16s: 2 iterations and 16 subsets; ^{99m}Tc: technetium-99m; CR: contrast recovery; CT: computed tomography; EANM: European Association of Nuclear Medicine; FOV: field of view; GC: gamma camera; LEHR: low energy, high resolution; NEMA IEC: National Electrical Manufacturers Association International Electrotechnical Commission; NM: nuclear medicine; OSEM: ordered subset expectation maximization; PET: positron emission tomography; PMT: photomultiplier tube; ROI: region of interest; SPECT: single-photon emission computed tomography; VOI: volume of interest

Declarations

Ethics approval and consent to participate

Not applicable

Consent for publication

Not applicable

Availability of data and materials

SPECT and CT raw datasets are available from the corresponding author on reasonable request.

Competing interests

The authors declare that they have no competing interests.

Funding

The research leading to these results has not received any external funding.

Authors' contributions

Study conception: Lina Vieira (LV); methodology: LV, Maria I.R. Gonçalves (MIG), Rui Parafita (RP), Mauro Costa (MC), Ana Geão (AG) and Edgar Pereira (EP); software and validation 3D Slicer: MC and MIG. The first draft of the manuscript was written by MIG.; supervision by LV and RP. All authors have read and agreed to the published version of the manuscript

Acknowledgements

H&TRC author gratefully acknowledge the FCT/MCTES national support through the UIDB/05608/2020 and UIDP/05608/2020.

Author details

[1]ISEL - Instituto Superior de Engenharia de Lisboa, Instituto Politécnico de Lisboa, 1959-007 Lisbon, Portugal. [2]Champalimaud Clinical Centre, Champalimaud Foundation, 1400-038 Lisbon, Portugal. [3]Hospital CUF Descobertas, 1998-018 Lisbon, Portugal, [4]Nuclearmed, HPA - Hospital Particular de Almada, 2800-455 Almada, Portugal. [5]H&TRC - Health & Technology Research Center, ESTeSL - Escola Superior de Tecnologia da Saúde, Instituto Politécnico de Lisboa, 1990-096 Lisbon, Portugal.

References

1. Noori-Asl M. Investigation of Different Factors Affecting the Quality of SPECT Images: A Simulation Study. J Med Phys. 2020 Mar;45(1):44-51. doi: 10.4103/JMP.JMP_88_19.
2. Cherry S, Sorenson J, Phelps M. Physics in Nuclear Medicine. 4th ed. Philadelphia: Elsevier Saunders; 2012. 544 p.
3. Loja MAR, Craveiro DS, Vieira L, Rodrigues JA, Portal R. Radiotherapy-customized head immobilization masks: from modeling and analysis to 3D printing. Nucl Sci Tech. 2019, 30(9), doi:142 10.1007/s41365-019-0667-2.
4. Myint TT, Ekjeen T, Wiyaporn K, Chaichana A, Vichianin Y, Tipparoj R, et al. A phantom study of factors afecting standardized uptake value (SUV) measurement of quantitative Tc-99m MDP bone SPECT/CT. Int J Appl Biomed Eng. 2019;12(1):20-5.
5. Zimmerman BE, Grošev D, Buvat I, Coca Pérez MA, Frey EC, Green A, et al. Multi-centre evaluation of accuracy and reproducibility of planar and SPECT image quantification: An IAEA phantom study. Z Med Phys. 2017 Jun;27(2):98-112. doi: 10.1016/j.zemedi.2016.03.008.
6. Dickson JC, Tossici-Bolt L, Sera T, de Nijs R, Booij J, Bagnara MC, et al. Proposal for the standardisation of multi-centre trials in nuclear medicine imaging: prerequisites for a European 123I-FP-CIT SPECT database. Eur J Nucl Med Mol Imaging. 2012 Jan;39(1):188-97. doi: 10.1007/s00259-011-1884-z.
7. Chilra P, Gnesin S, Allenbach G, Monteiro M, Prior JO, Vieira L, Pires Jorge JA. Cardiac PET/CT with Rb-82: optimization of image acquisition and reconstruction parameters. EJNMMI Phys. 2017 Dec; 4(1): 10. doi: 10.1186/s40658-017-0178-3.
8. Tatsch K. Standardisation and harmonisation boost the credibility of nuclear medicine procedures. Eur J Nucl Med Mol Imaging. 2012 Jan;39(1):186-7. doi: 10.1007/s00259-011-1996-5.
9. Hughes T, Shcherbinin S, Celler A. A multi-center phantom study comparing image resolution from three state-of-the-art SPECT-CT systems. J Nucl Cardiol. 2009 Dec;16(6):914-26. doi: 10.1007/s12350-009-9132-7.

10. Hughes T, Celler A. A multivendor phantom study comparing the image quality produced from three state-of-the-art SPECT-CT systems. Nucl Med Commun. 2012 Jun;33(6):663-70. doi: 10.1097/MNM.0b013e328351d549.
11. Peters SMB, van der Werf NR, Segbers M, van Velden FHP, Wierts R, Blokland KJAK, et al. Towards standardization of absolute SPECT/CT quantification: a multi-center and multi-vendor phantom study. EJNMMI phys. 2019 Dec;6(1):29. doi: 10.1186/s40658-019-0268-5.
12. Peters SMB, Meyer Viol SL, van der Werf NR, de Jong N, van Velden FHP, Meeuwis A, et al. Variability in lutetium-177 SPECT quantification between different state-of-the-art SPECT/CT systems. EJNMMI Phys. 2020 Feb;7(1):9. doi: 10.1186/s40658-020-0278-3.
13. Kupitz D, Wissel H, Wuestemann J, Bluemel S, Pech M, Amthauer H, et al. Optimization of SPECT/CT imaging protocols for quantitative and qualitative 99mTc SPECT. EJNMMI Phys. 2021 Jul;8(1):57. doi: 10.1186/s40658-021-00405-3.
14. Alqahtani MM, Willowson KP, Constable C, Fulton R, Kench PL. Optimization of 99mTc whole-body SPECT/CT image quality: A phantom study. J Appl Clin Med Phys. 2022 Apr;23(4):e13528. doi: 10.1002/acm2.13528.
15. Boellaard R, Delgado-Bolton R, Oyen WJ, Giammarile F, Tatsch K, Eschner W, et al. European Association of Nuclear Medicine (EANM). FDG PET/CT: EANM procedure guidelines for tumour imaging: version 2.0. Eur J Nucl Med Mol Imaging. 2015 Feb;42(2):328-54. doi: 10.1007/s00259-014-2961-x.
16. Greer KL, Scarfone C. SPECT phantom user's manual. Hillsborough: Data Spectrum Corporation; 2001.
17. Greer K. NEMA IEC body phantom set™ user's manual. Hillsborough: Data Spectrum Corporation; 2008.
18. National Electrical Manufacturers Association. Performance Measurements of Positron Emission Tomographs. Virginia: NEMA; 2018. 49 p. NEMA Standards Publication NU 2-2018.
19. Fedorov A, Beichel R, Kalpathy-Cramer J, Finet J, Fillion-Robin JC, Pujol S, et al. 3D Slicer as an image computing platform for the Quantitative Imaging Network. Magn Reson Imaging. 2012 Nov;30(9):1323-41. doi: 10.1016/j.mri.2012.05.001.
20. DePuey EG. Advances in SPECT camera software and hardware: currently available and new on the horizon. J Nucl Cardiol. 2012 Jun;19(3):551-81. doi: 10.1007/s12350-012-9544-7.
21. Frey EC, Humm JL, Ljungberg M. Accuracy and Precision of Radioactivity Quantification in Nuclear Medicine Images. Semin Nucl Med. 2012 May;42(3):208-18. doi: 10.1053/j.semnuclmed.2011.11.003.
22. ALehyani SHA. Application of single photon emission computed tomography (SPECT) parameters for bone scintigraphy. J King Saud Univ Sci . 2009 Aug;21(2):109-17. doi: 10.1016/J.JKSUS.2009.07.004.
23. Lyra M, Ploussi A. Filtering in SPECT Image Reconstruction. Int J Biomed Imaging. 2011 Apr;2011:1-14. doi: 10.1155/2011/693795.
24. Saha GB. Performance Parameters of Gamma Cameras. In: Saha GB, editor. Physics and Radiobiology of Nuclear Medicine. 3rd ed. New York: Springer; 2006. p. 118-38.
25. Yusof MFM, Solehah U, Ghani A, Ghazali NA, Khaizul AT, Idris AW. Evaluation of contrast and recovery coefficients as performance parameters in planar and SPECT imaging. Mater Sci Eng. 2020;785. doi: 10.1088/1757-899X/785/1/012046.
26. Vieira L. Contributo para a optimização dos estudos de perfusão miocárdica utilizando imagens de medicina nuclear sincronizadas com o electrocardiograma [dissertation on the Internet]. Lisboa: Faculdade de Ciências da Universidade de Lisboa; 2010 [cited 2021 Nov 4]. Available from: http://hdl.handle.net/10451/4500.
27. Khalil M, editor. Basic Sciences of Nuclear Medicine. 1st ed. Berlin: Springer; 2011. 423 p.
28. Lima JJP de. Física em medicina nuclear: temas e aplicações. Coimbra: Imprensa da Universidade de Coimbra; 2008. 566 p.
29. Ritt P, Vija H, Hornegger J, Kuwert T. Absolute quantification in SPECT. Eur J Nucl Med Mol Imaging. 2011 May;38 Suppl 1:S69-77. doi: 10.1007/s00259-011-1770-8.
30. Knoll P, Kotalova D, Köchle G, Kuzelka I, Minear G, Mirzaei S, et al. Comparison of advanced iterative reconstruction methods for SPECT/CT. Z Med Phys. 2012 Feb;22(1):58-69. doi: 10.1016/j.zemedi.2011.04.007.